

# Holographic spatial walk-off polarizer and its application to a 4-port polarization-independent optical circulator

Jing-Heng Chen and Der-Chin Su

Institute of Electro-Optical Engineering, National Chiao Tung University, 1001 Ta Hsueh Road, Hsin-Chu 30050, Taiwan, R.O.C.  
[t7503@faculty.nctu.edu.tw](mailto:t7503@faculty.nctu.edu.tw)

Jung-Chieh Su

Industrial Technology Research Institute, Opto-Electronics & Systems Laboratories,  
Bldg-78 N000, 195-8 Chung Hsing Road, Sec.4, Chutung 31041, Hsin-Chu, Taiwan, R.O.C.

**Abstract:** Based on the coupled-wave theory, a holographic spatial walk-off polarizer (HSWP) is designed. This HSWP is a transmission-type phase volume holographic grating on a substrate and its optical recording geometry can be derived from Chen's corrected methodology with a desired reconstruction condition. A pair of fabricated HSWPs with the splitting angle of  $60^\circ$  is applied to assemble a new type of 4-port polarization-independent optical circulator. The operating principles and the characteristics of the proposed HSWP and the prototype optical circulator are discussed.

©2003 Optical Society of America

**OCIS codes:** 060.4510 (Optical communications); 090.2890 (Holographic optical elements); 260.5430 (Polarization).

---

## References and links

1. R. Ramaswami, K. N. Sivarajan, *Optical networks*, second ed., Morgan Kaufmann, San Francisco, 2002, p. 112-115 (Chapter 3).
2. K. Muro, K. Shiraishi, "Poly-Si/SiO<sub>2</sub> laminated walk-off polarizer having a beam-splitting angle of more than 20°," *J. Lightwave Technol.* **16**, 127-133 (1998).
3. J. Hecht, *Understanding fiber optics*, fourth ed., Prentice Hall, New Jersey, 2002, P. 346-350 (Chapter 14).
4. L. D. Wang, "High-isolation polarization-independent optical quasi-circulator with a simple structure," *Opt. Lett.* **23**, 549-551 (1998).
5. Y. K. Chen et al. "Low-crosstalk and compact optical add-drop multiplexer using a multiport circulator and fiber Bragg gratings," *IEEE Photon. Technol. Lett.* **12**, 1394-1396 (2000).
6. J. Nicholls, "Birefringent crystals find new niche in WDM networks," *WDM SOLUTIONS* **3**, 33-36 (2001).
7. J. Liu and R. T. Chen, "Path-reversed substrate-guided-wave optical interconnects for wavelength-division demultiplexing," *Appl. Opt.* **38**, 3046-3052 (1999).
8. R. Shechter, Y. Amitai, and A. A. Friesem, "Compact wavelength division multiplexers and demultiplexers," *Appl. Opt.* **41**, 1256-1261 (2002).
9. H. Kogelnik, "Coupled wave theory for thick hologram gratings," *Bell Syst. Tech. J.* **48**, 2909-2947 (1969).
10. J. H. Chen, D. C. Su, J. C. Su, "Shrinkage- and refractive-index shift-corrected volume holograms for optical interconnects," *Appl. Phys. Lett.* **81**, 1387-1389 (2002).
11. B. J. Chang, C. D. Leonard, "Dichromated gelatin for the fabrication of holographic optical elements," *Appl. Opt.* **18**, 2407-2417 (1979).
12. D. G. McCauley, C. E. Simpson, W. J. Murbach, "Holographic optical element for visual display applications," *Appl. Opt.* **12**, 232-242 (1973).
13. B. J. Chang, Optical information storage, *Proc. SPIE* **177**, 71-81 (1979).

## 1. Introduction

A spatial walk-off polarizer (SWP) [1, 2] capable of splitting an optical beam into two orthogonally polarized parallel beams is an important optical component for fabricating the fiber-optic isolators and circulators [3-5] widely used in optical communication systems. A conventional SWP is made of a birefringence crystal [6] or a transparent substrate coated with multi-layer high/low-index materials [2]. The separation between the two orthogonally polarized beams produced by these conventional methods is typically limited by the small splitting angle and the cost may be still too high. A volume holographic grating has special functions and high efficiency, so it is always used as an alternative element, especially in the category [7, 8] of optical communications. In this paper, a new type of spatial walk-off polarizers based on the transmission-type phase volume holographic grating [9] is proposed. To demonstrate the feasibility of the idea, some sample holographic SWPs (HSWPs) are designed by using the coupled-wave theory [9] and fabricated with the conventional holographic recording geometry under the conditions derived from Chen's corrected methodology [10]. The HSWPs are designed for the 1300nm wavelength and were fabricated with an He-Cd laser at the wavelength of 441.6nm and with the dichromated gelatin (DCG) as the recording material [11, 12]. The fabricated HSWPs have a larger splitting angle of  $60^\circ$  and the demonstrated diffraction efficiencies of the s- and p- polarized components are 3% and 90% respectively, limited by our experimental conditions. With a pair of fabricated HSWPs, a new type of 4-port polarization-independent optical circulator is designed by modifying the configuration of a 4-port quasi-optical circulator described by Nicholls [6]. The characteristics of the HSWPs as well as the operating principle and the performance of the proposed optical circulator will be discussed in the following sections.

## 2. Holographic spatial walk-off polarizer

The holographic spatial walk-off polarizer (HSWP) is a transmission-type phase volume holographic grating on a substrate, as shown in Fig. 1. Its grating structure is designed in such a way that either of the s- or p- polarized component of a normal incident beam at A is transmitted straight through the grating and the substrate while the other orthogonally polarized component is completely diffracted into the substrate with a diffraction angle  $\theta_{s2}$  which is larger than the critical angle  $\theta_c$  at the substrate-air interface. In this way, the diffracted beam is totally reflected at point B and hits the grating again at point C. This beam is totally reflected at point C, and the reflected beam from point C satisfies the Bragg condition [9] of the grating. The propagation direction of the reflected beam is in parallel to that of the beam diffracted by the grating at point A. Because the structure of the grating at point C is the same as that at point A, the diffracted beam at point C will be in parallel to the input beam at point A; that is, the output beam passes normally through the substrate. The detail of the beam propagation at point C is shown in the upper left circle of Fig. 1. Consequently, two orthogonally polarized parallel beams with the separation of length AC can be obtained.

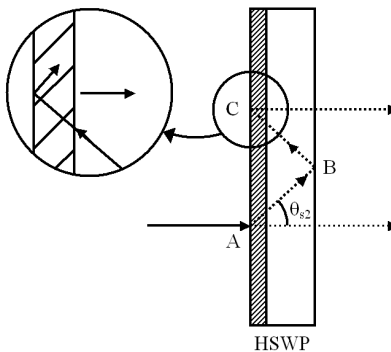


Fig. 1. Structure and operation principle of the holographic spatial walk-off polarizer.

### 2.1 Diffraction efficiency of an HSWP

Because the incident angle of the input beam is set to be 0, the diffraction efficiencies of this grating for s- and p- polarized components can be derived from the coupled-wave theory [9] and can be respectively written as

$$\eta_s = \sin^2 \left[ \frac{\pi n_1 d}{\lambda_r} \frac{1}{(\cos \theta_d)^{1/2}} \right] = \sin^2 \nu_s, \quad (1)$$

and

$$\begin{aligned} \eta_p &= \sin^2 \left[ \frac{\pi n_1 d}{\lambda_r} \frac{1}{(\cos \theta_d)^{1/2}} \cos \theta_d \right] \\ &= \sin^2 (\nu_s \cos \theta_d) = \sin^2 \nu_p. \end{aligned} \quad (2)$$

Here  $\theta_d$  is the diffraction angle in the phase volume grating,  $n_1$  is the index modulation strength,  $d$  is the hologram emulsion thickness, and  $\lambda_r$  is the reconstruction wavelength. For our applications, the necessary condition for this grating to satisfy is that either  $\eta_s$  or  $\eta_p$  is 100% and the other one is zero.

### 2.2 Optical recording and reconstruction geometry

The optical configuration for recording and reconstructing the transmission-type phase volume holographic grating is shown in Fig. 2. Two light beams  $R_1$  and  $S_1$  with wavelength  $\lambda$  are incident on a recording material at  $\theta_{r1}$  and  $\theta_{s1}$ . The recording material consists of a substrate and a photographic emulsion with refractive index  $n_{f1}$  (at  $\lambda$ ) and thickness  $d_1$ . After the exposure, the recording material is post-processed for developing. The thickness of the photographic emulsion shrinks to  $d$  after developing. The reconstructed light  $R_2$  with wavelength  $\lambda_r$  is incident normally (i.e.,  $\theta_{r2}=0^\circ$ ), and the outgoing wave  $S_2$  with diffracted angle  $\theta_{s2} = \sin^{-1} \left[ \frac{n_{f2}}{n_s} \sin \theta_d \right]$  in the substrate. Here  $n_s$  and  $n_{f2}$  are the refractive indices of the

substrate and the processed photographic emulsion at  $\lambda_r$  respectively. The values of the recording conditions  $\theta_{r1}$  and  $\theta_{s1}$  can be calculated by using Chen's corrected methodology [10] under the experimental conditions in which  $\lambda$ ,  $\lambda_r$ ,  $n_{f1}$ ,  $d_1$ ,  $n_{f2}$ ,  $d$ ,  $\theta_{r2}$  and  $\theta_{s2}$  are specified.

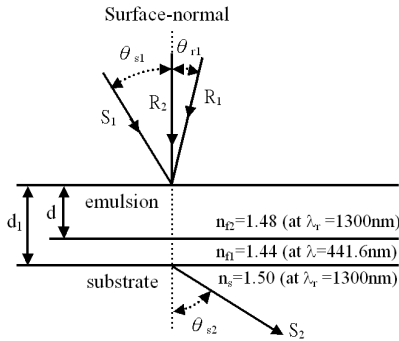


Fig. 2. Geometry for recording and reconstruction the transmission-type phase volume holographic grating considering the thickness and refractive index shifts after optical exposure and post-processing.

### 2.3 Fabrications and results

In order to demonstrate the validity of our design, several HSWPs for 1300 nm wavelength are fabricated. An He-Cd laser with wavelength  $\lambda = 441.6$  nm is used for exposure and the

dichromated gelatin (DCG) is used as the recording material. We prepare the DCG recording material with the processes proposed by McCauley et al. [12]. Since in general it is difficult to fabricate DCG with  $n_1 > 0.08$  [11], so we first substitute the specifications  $d=17\mu\text{m}$  and  $n_1 < 0.08$ ,  $\theta_{s2} > \theta_c (\cong 41.8^\circ)$ , and  $\lambda_r=1300\text{nm}$  into Eqs. (1) and (2) under the necessary condition described in **Sec. 2.1**. The results we get are  $\theta_d=60^\circ$  and  $n_1=0.054$ . Next, the recording conditions  $\theta_{r1}=14.1^\circ$  and  $\theta_{s1}=32.6^\circ$  are obtained by substituting the experimental conditions  $\lambda=441.6\text{nm}$ ,  $\lambda_r=1300\text{nm}$ ,  $d_1=22\mu\text{m}$ ,  $n_{f1}=1.44$  (at  $\lambda=441.6\text{nm}$ ),  $d=17\mu\text{m}$ ,  $n_{f2}=1.48$  (at  $\lambda_r=1300\text{nm}$ ),  $\theta_{r2}=0^\circ$ , and  $\theta_{s2}=58.7^\circ$  (i.e.,  $\theta_d=60^\circ$ ) into Chen's corrected methodology. After exposure and post-processing, the HSWPs are obtained and their diffraction efficiencies are measured to be  $\eta_s=3\%$  and  $\eta_p=90\%$ . The separation between the two orthogonally parallel beams is 3.2 mm.

### 3. A new type of 4-port polarization-independent optical circulator

As shown in Fig. 3, an alternative type of 4-port polarization-independent optical circulator with a pair of our fabricated HSWPs is designed by modifying the configuration of an optical quasi-circulator described by Nicholls [6]. Besides the HSWPs, this optical circulator consists of four reflection prisms (RPs), six polarization-beam splitters (PBSs), a  $45^\circ$  Faraday rotator (FR), and a  $45^\circ$  half-wave plate (H). The two identical HSWPs face the opposite directions as shown in the figure. If an input beam is normally incident on HSWP<sub>1</sub> from Port 1 as shown in Fig. 3(a), then the s-polarized component passes through HSWP<sub>1</sub> directly and the p-polarized component also passes through HSWP<sub>1</sub> after two diffractions and two total-reflections. Next, these two orthogonally polarized components pass through FR and H. Their states of polarization (SOP) are rotated a total of  $90^\circ$ ,  $+45^\circ$  by FR and  $+45^\circ$  by H. For easy understanding, a circle with a bisecting line is used to represent the associated SOP of the light after propagating through each component. Symbols  $\ominus$  and  $\oplus$  represent the electric-field lies in the planes perpendicular (s-polarization) and parallel (p-polarization) to the paper plane respectively, and the symbol  $\oplus$  represents the light beam has both s- and p-polarized components. The beams finally enter HSWP<sub>2</sub> and then recombine together with the similar diffraction and total-reflection effects in HSWP<sub>1</sub> and reach Port 2.

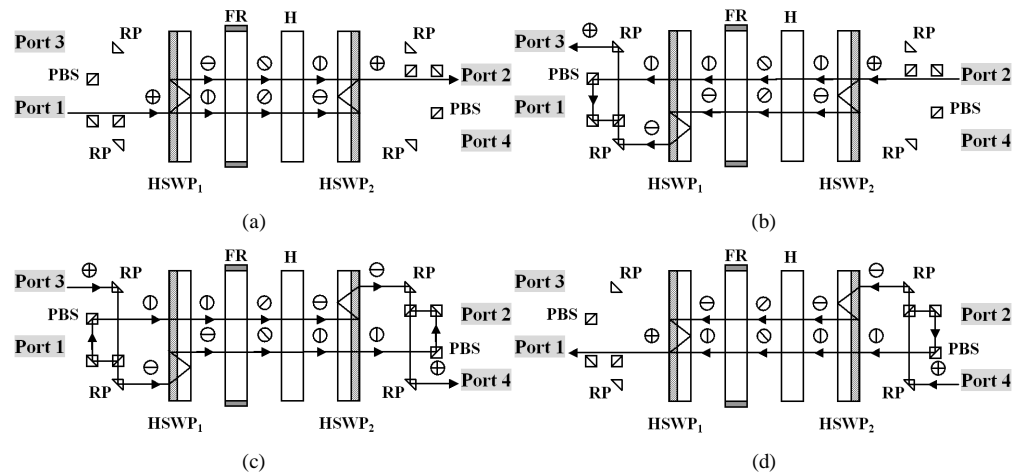


Fig. 3. Structure and operation principles of the proposed 4-port polarization independent optical circulator.

On the other hand, if an input beam is incident normally on HSWP<sub>2</sub> from Port 2 as shown in Fig. 3(b), then the s-polarized component passes through HSWP<sub>2</sub> directly, and the p-polarized component also passes through HSWP<sub>2</sub> after two diffractions and two total-reflections. These two orthogonally polarized components pass through H and FR. Their

SOPs are rotated  $-45^\circ$  by H and  $+45^\circ$  by FR, a total of  $0^\circ$ . The s-polarized component passes through HSWP<sub>1</sub> and is reflected by three PBSs and one PR, and enters Port 3. The p-polarized component is diffracted and total-reflected similarly in HSWP<sub>1</sub> and propagates through one RP, one PBS, and another RP. Finally, it arrives at Port3 and recombines with the s-polarized component. Two other similar operations for the routes of Port 3→Port 4 and Port 4→Port 1 can be done with the introduction of additional RPs and PBSs, as shown in Fig. 3 (c) and (d) respectively. If the PBSs are located accurately in the configurations of Fig. 3(b) and (d), there will be no optical path difference between s- and p- polarizations for any route. Hence, this optical circulator can function as a polarization-independent 4-port optical circulator without polarization mode dispersion (PMD).

A prototype of the 4-port optical circulator is assembled with a pair of fabricated HSWPs, a Faraday rotator and a half wave-plate. The transmittances of FR and H are 0.95 and 0.97, respectively. The parameters of this prototype device can be estimated from the diffraction efficiencies of HSWPs and the transmittances of FR and H. The estimated results are listed in Table I(a). Because  $\eta_s$  and  $\eta_p$  of our fabricated HSWPs are slightly different from the theoretical values, the transmittances of two orthogonally polarized components are slightly different in the routes of Port 2→Port 3 and Port 4→Port 1.

Table 1. Associated losses and isolation<sup>a</sup> (in Decibels) of 4-port circulator with wavelength 1300nm by using (a) fabricated HSWPs; and (b) HSWPs with ideal diffraction efficiencies  $\eta_s < 1\%$  and  $\eta_p > 99\%$  and predicted anti-reflection coatings.

(a)				
In Port	Out Port			
	1	2	3	4
1	14.26 <sup>b</sup>	2.09 <sup>c</sup>	47.91	14.18
2	11.91	14.26 <sup>b</sup>	2.02 <sup>c</sup>	47.91
3	28.24	14.15	14.26 <sup>b</sup>	2.09 <sup>c</sup>
4	2.02 <sup>c</sup>	28.24	44.92	14.26 <sup>b</sup>

(b)				
In Port	Out Port			
	1	2	3	4
1	>30 <sup>b</sup>	<0.50 <sup>c</sup>	>73.06	>23.43
2	>20.42	>30 <sup>b</sup>	<0.50 <sup>c</sup>	>73.06
3	>53.11	>23.38	>30 <sup>b</sup>	<0.50 <sup>c</sup>
4	<0.50 <sup>c</sup>	>53.11	>53.43	>30 <sup>b</sup>

<sup>a</sup>All values without a superscript are isolation values;

<sup>b</sup>Return losses; <sup>c</sup>Insertion losses.

#### 4. Discussion

Since our fabricated HSWPs have no anti-reflection coatings, there is about 4% reflection loss at each boundary. If they are anti-reflection coated, then the reflection losses should be decreased to 0.1%. In addition, if the holographic exposure and the post-processing procedure are controlled more accurately, the HSWPs may have the theoretical diffraction efficiencies [13], i.e.,  $\eta_s \cong 0\%$  and  $\eta_p \cong 100\%$ . Under these two possible improved conditions, the performance of this 4-port optical circulator can be enhanced greatly, and the associated parameters are calculated and listed in Table I(b) with  $\eta_s < 1\%$  and  $\eta_p > 99\%$ . Moreover, if  $K$  and  $\Delta\lambda$  are the magnitude of grating vector  $\vec{K}$  and the wavelength shift with respect to the central wavelength  $\lambda_r$ , the diffraction efficiencies of a transmission-type phase volume hologram for the s- and p-polarization states near the Bragg condition are given as [9]

$$\eta_i = \frac{\sin^2(\sqrt{v_i^2 + \xi^2})}{(1 + \xi^2/v_i^2)} \quad (i = s, p), \quad (3)$$

with

$$\xi = \frac{-\Delta\lambda K^2 d}{8\pi n_{f2} \cos\theta_d}, \quad (4a)$$

$$K = \left(\frac{4\pi n_{f2}}{\lambda_r}\right) \cdot \sin\frac{\theta_d}{2}. \quad (4b)$$

Substituting our experimental conditions  $n_1=0.054$ ,  $d=17\mu\text{m}$ ,  $\lambda_r=1300\text{nm}$ ,  $\theta_d=60^\circ$ , and  $n_{f2}=1.48$  (at  $\lambda_r=1300\text{nm}$ ) into Eq. (3), the theoretical curves of diffraction efficiencies versus wavelengths for our HSWP is shown in Fig. 4. It is obvious that the bandwidth with  $\eta_p>90\%$  and  $\eta_s\approx 0\%$  at  $1300\text{nm}$  central wavelength is as large as  $20\text{nm}$ . It should also be possible to design the central wavelength to be at  $1550\text{ nm}$  wavelength range.

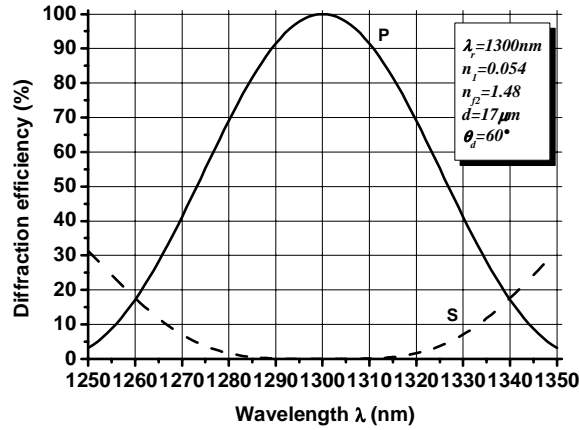


Fig. 4. Calculated diffraction efficiencies of the HSWP versus wavelength at  $1300\text{nm}$  central wavelength.

## 5. Conclusions

A new type of spatial walk-off polarizer has been proposed in this paper. It is essentially a transmission-type phase volume holographic grating on a substrate and can be fabricated by conventional holographic exposure methods. The demo HSWPs designed for  $1300\text{ nm}$  wavelength have been fabricated with the DCG recording material and an He-Cd laser at  $441.6\text{ nm}$  wavelength. They have a larger splitting angle of  $60^\circ$  and the diffraction efficiencies of  $\eta_s=3\%$  and  $\eta_p=90\%$ . A new type of 4-port polarization-independent optical circulator composed of a pair of HSWPs has also been proposed and demonstrated.

## Acknowledgements

This research was supported in partial by a grant from Lee & MTI Center for Networking at the National Chiao Tung University, Taiwan, R. O. C.